

## Tracking Individual Particles in a Fluidized Bed using a Medical PET-Camera

Hoffmann, A.C.<sup>1</sup>, Dechsiri, C.<sup>2,3</sup>, van de Wiel, F.<sup>3</sup>, Ghione, A.<sup>1</sup>, Dehling, H.G.<sup>4</sup>, Paans, A.M.J.<sup>5</sup>

1. Department of Physics, Bergen, 5007, Norway
2. Department of mathematics, Groningen, 9747 AC, The Netherlands
3. Stratingh Institute, Groningen, 9747 AG, The Netherlands
4. Fakultät für Mathematik, Bochum, 44780, Germany
5. PET Center, Groningen University Hospital, Groningen, 9700 RB, The Netherlands

**Keywords** Positron emission tomography; lines of response; fluidized bed; single particle motion.

### ABSTRACT

*This paper describes a series of experiments tracing a single radioactive particle in a fluidized bed in an ECAT EXACT HR+ PET camera in order to obtain 3-D paths for an actual bed particle – i.e. a particle typical for the bed material – with a high spatial and temporal resolution. The paper describes how "lines of response" (LORs) were calculated from the binary list-mode files from the camera, and how particle positions (1 per ms) were computed from the LORs. It also gives a condensed account of how the data were analyzed further. The particle movement in the bed is shown graphically, and the findings interpreted in light of the theories on mechanisms behind particle movement in fluidized beds. Among other things the issue of fast, short-range movement of particles in fluidized beds is discussed. The findings are consistent with the notion of upward particle motion in the wakes of fluidization bubbles, and downward motion in the bulk. The vertical motion is rather structured and is cyclical, vertical paths often spanning most of the bed. The lateral motion is less structured. A close analysis of the spread in the millisecond positions both for the fixed and fluidized bed does not reveal any fast, short-range motion of the particles in the fluidized condition.*

### 1 INTRODUCTION

Positron emission tomography (PET) and "positron emission particle tracking" (PEPT) are new techniques for visualizing the particle movement in process equipment. These techniques make direct tracking of particle pulses or of individual particles possible in processes, for instance in fluidized beds. Much of the pioneering work in this has been done at the University of Birmingham (e.g. Snieders et al. 1999, Stein et al., 2000), and subsequently also the Technical University of Delft. One limitation in these techniques was the size of the tracer particle, which had to be relatively large to be given sufficient activity for tracking. It was possible to use a pellet of the same bulk density as the bed material, which was shown to behave similarly to the bed particles themselves (e.g. Snieders et al., 1999).

The objective of this work was to achieve tracking of a single tracer particle typical for the bed material with high temporal and spatial resolution, to answer questions about the nature of – and flow patterns in – fluidized beds and the transport mechanisms for particles in them.

The most advanced cameras for Positron Emission Tomography can often be found in the medical sector. The associated software, however, is geared to medical applications, so when using the equipment for process characterization, the basic camera output needs to be analyzed directly. Cooperation with the University Hospital in Groningen (AZG) made it possible to make use a state-of-the-art ECAT EXACT HR+ PET camera, by constructing a fluidized bed to fit in the cylindrical measuring region of the camera.

### 2 EXPERIMENTS AND DATA ANALYSIS

The work reported here formed part of a larger experimental plan to study the dynamics of both tracer pulses and of individual particles for elucidating stochastic models for particle dynamics in fluidized beds. The experimental technique, both that of PET in general, and the one used in this work is described in some detail elsewhere (e.g. Dechsiri et al. 2002). In this paper we will therefore concentrate on the analysis of the data emanating from the single particle experiments. It suffices to

say that the particles used were a macroporous anion-exchange resin (MP500), which could easily be labeled with the radioactive tracer. The labeling was done by soaking the particles briefly in a fluoride containing solution to allow the negative F-ions, including some  $^{18}\text{F}$  ions produced in a cyclotron under the laboratory, to exchange with the Cl ions in the resin. The particles were then dried in a fluidized bed. The particle diameter was  $470\ \mu\text{m}$ , the envelope density  $1060\ \text{kg/m}^3$ , and the measured minimum fluidization velocity was  $0.134\ \text{m/s}$ . In all three experiments the fluidization velocity was  $0.150\ \text{m/s}$ .

A cylindrical glass column was used, with height 35 cm and diameter 15 cm. These dimensions were chosen to fit the column in the PET scanner. Both on the top and on the bottom of the column sintered plates were mounted. The sintered plate at the top prevented the particles from exiting the bed. The porosity of the top plate was high, while that of the low one was low to improve the gas distribution.

The PET technique is based on the radioactive decay of a radioactive labeler, here  $^{18}\text{F}$ , which leads to the emission of a positron and neutrino. The positron travels a few mm through the system before annihilating with an electron. For energy conservation this annihilation normally results in the back-to-back emission of two photons, in this case of 511 keV.

The emitted photons are detected by cylindrically arranged sensors consisting of 72 blocks, each arrayed in  $8 \times 8$  detectors. In depth there are 4 such rings of blocks, giving  $4 \times 72 \times 64$  detectors in total. A sketch of the arrangement (with fewer blocks) is shown in Figure 1A. If two detections are within a narrow time window, they are adjudged to have emanated from the same annihilation, and a "line of response" (LOR) is drawn between them, the position of which is stored as

- its distance (in number of detectors) to the camera center,
- its angle (also in number of detectors) with the vertical, and
- the number of the two detectors in the direction normal to the paper.

All this is stored in binary form, in buffers of 32 32-bit words, which had to be read and deciphered.

Space does not allow us to account for the structure of the binary output, or for the conversion of these data to LOR coordinates. We intend to do this in more detailed papers under preparation. It suffices to say that coordinates for the two detectors for each LOR were determined using a Cartesian coordinate system with the z-direction normal to the paper in Figure 1.

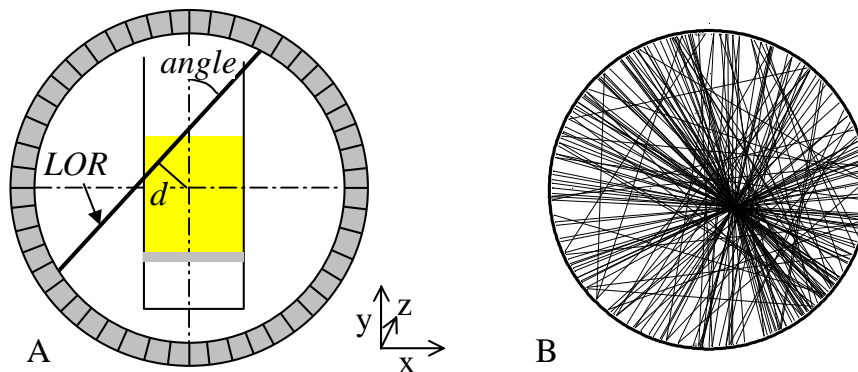


Figure 1. A: Sketch of the bed arrangement within the cylindrical detection zone of the camera, detector blocks and an LOR with its defining parameters are sketched. B: about 150 LORs from one ms.

About 500 LORs were detected each millisecond (ms), 150 LORs from one ms are shown in Figure 1B. It is evident that some of the LORs are "bad". This can be due to a number of factors. One is the possibility that two annihilation events take place within the same time window, each with one end of the LOR within the detector array, and the other end falling outside. The camera will interpret this as one event. Although most of the LORs cross in one point, and are therefore "good", there is also some scatter in those. There are four reasons for this:

1. The finite size of the detectors limits spatial resolution, and therefore the LOR precision.
2. The positron travels a few mm before annihilating with an electron
3. The emission of photons may not be exactly collinear, i.e.  $180^\circ$  apart, this depends on the momentum of the electron-positron pair before the annihilation
4. The tracer particle itself has finite dimensions.

The procedure was to eliminate the bad LORs and determine the particle position by averaging the cutpoints between the rest. It was decided to determine one particle position per ms. Computing power was a limiting factor for the analysis, the number of operations for computing particle positions increase with the square of the LORs included in the analysis. Writing a program in a compiled language (Pascal), made it possible to include 100 LORs per ms. The most efficient algorithm was one of “zeroing in” on the average of the good cutpoints by successive elimination of bad cutpoints. The position data were generated in a Cartesian coordinate system, which is convenient for viewing projections on the coordinate planes. Some results will be shown in cylindrical coordinate systems in subsequent publications.

### 3 RESULTS

In the following sections we show different aspects of the results. We start with the short time-scale motion, i.e. the individual ms points, study the standard deviation of the points in the static and fluidized conditions, and try to detect any fast, short-range motion of the fluidized particles. Thereafter we consider the particle motion on a longer time scale and relate this to the particle transport mechanisms envisaged in fluidized beds.

#### 3.1 Precision of the data and short time-scale particle motion

The particle tracking was initiated about 10 seconds before the bed was fluidized, making it possible to ascertain the spread in the ms positions due to experimental error only. Figure 2 A and B show ms positions during periods where the bed was unfluidized and fluidized, respectively.

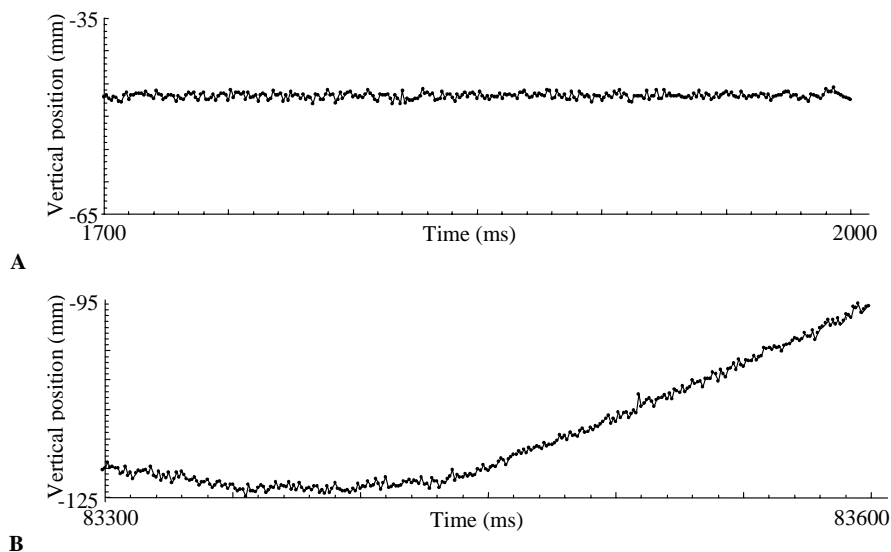


**Figure 2 A and B ms vertical particle positions (y-coordinate) in the unfluidized and the fluidized state, respectively**

To quantify the precision with which the particle's position can be determined per ms, we determined the standard deviation in the data corresponding to the unfluidized state while using different number of LORs per ms. Since the number of cutpoints between LORs increase with the square of the number of LORs we would expect the standard deviation of ms points to decrease linearly with number of LORs. In fact, it decreased less so, leading us to seek some source of scatter in addition to that incurred by the sources from the analysis alone, which were mentioned above. We are not sure which this source of scatter is at the present stage. Further data analysis may reveal this.

The standard deviation in the data shown in the Figure 2 A is  $485 \pm 6 \mu\text{m}$ , indicating that when using 100 LORs the particle position can be determined to within one particle diameter once per ms. The standard deviation in the x-coordinates was about the same, while that of the z-coordinate was three times as large. These standard deviations varied slightly between the experiments.

The motion of the particle in the fluidized bed is evident in Figure 2 B, and we shall return to this large-scale, long-term motion.

One question that arises is whether we can detect any short-range, fast particle movement which may be obscured by the scatter in the ms points. We can attempt to answer this question by comparing the standard deviation in the unfluidized state with that in the fluidized state. To do this, the particle motion in the fluidized bed was subdivided in small time segments of 10 ms, in which the path could be well fitted with a straight line, and the residual standard deviation determined. The resulting estimate of the scatter in the particle position in the fluidized state was  $0.487 \pm 9 \mu\text{m}$ , which is the same as in the unfluidized bed. We can, therefore, not detect any fast, short range motion of a single particle in a fluidized bed. With further work we should be able to make this type of comparison with higher statistical significance; also this comparison may not give the same result for all three experiments.

### 3.2 Long-term, large-scale particle motion

The plots of Figure 2 indicate that we can smooth the data over a number of ms reducing the scatter without losing information about the real motion of the particle. A preliminary study of the data indicates that the fastest motion of the particle will be faithfully reproduced if some running average spanning about 10 ms is calculated.

Kendall (1985) discusses the issue of doing this in an optimal way and also other useful methods for characterizing time series. For the time being we have simply determined the average over 10 ms. Figure 3 shows typical plots of the particle motion.

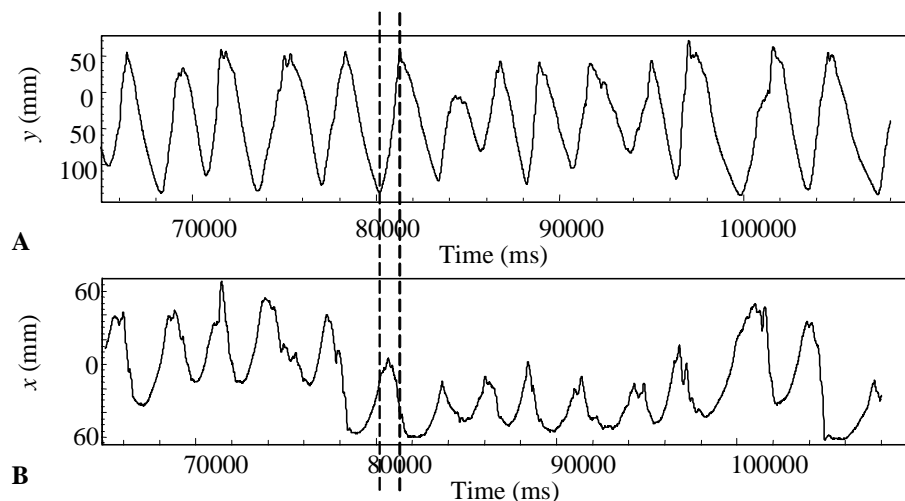


Figure 3 Time-series of the tracer particle's  $y$ -position (height in bed) and  $x$ -position

Several features can be noted. The bed was 19 cm high, and in the fluidized state about 25 cm. The top figure shows that the particle almost always traverses the entire length of the bed on its upward and downward motion, giving a regular, cyclic motion of the particle. It is also clear that the upward motion is faster in general than the downward one. Further the velocity of the downward motion appears in many cases to decrease right in the bottom section of the bed.

Comparing the two figures, it is clear that the upward motion is generally associated with a slight lateral motion towards higher  $x$ -coordinate, although the lateral motion is much less pronounced and more irregular than the vertical one.

To shed more light on the particle motion, we devised a way of identifying the individual upward and downward paths, their starting- and end points and the average velocity during each path. Since significant downward and upward paths alternate we can see these points as the transition points between upward and downward paths. They are shown in Figures 4 and 5, respectively.

Looking at of Figure 4 A we see that the lateral distribution of particle path starting points are not uniformly distributed over the bed cross-section, bearing witness to the fact that the aeration of the bed through the porous plate distributor was not ideal, a perennial problem with this type of distributor. The end points, on the other hand, are better distributed due to the fact that the bed was slightly inclined to the vertical to obtain the appearance of uniform fluidization.

The left hand plates show the vertical distribution of starting and end points for upward paths. As the previous figures also indicate we see that the starting and end points are concentrated in, but to some extent distributed over-, the bottom and top sections of the bed, respectively.

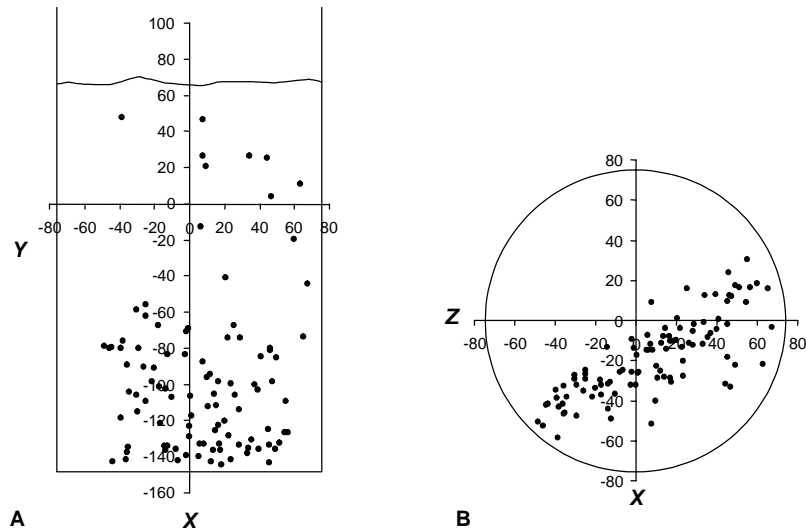


Figure 4 Starting points for upward particle paths, the approximate position of the bed is indicated

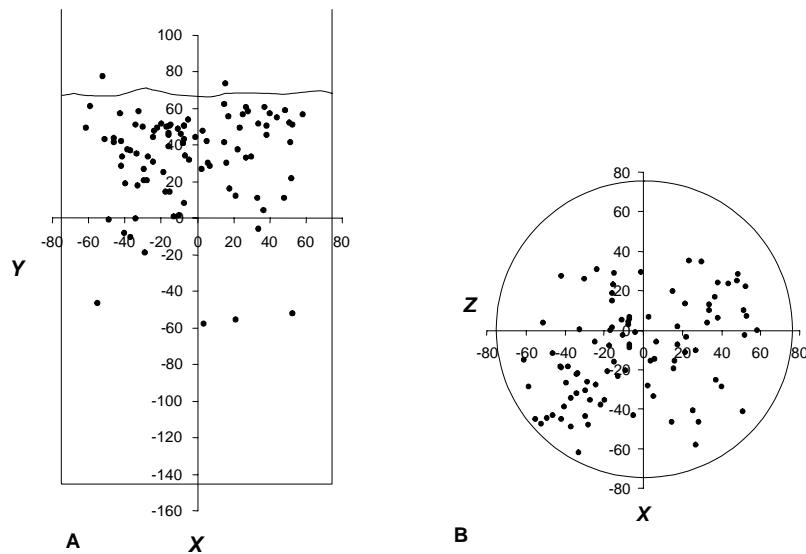


Figure 5 End points for upward particle paths

## 4 DISCUSSION

The apparent absence of fast, small-scale particle motion in the fluidized bed would be consistent with the visual observation that fluidized particles are surprisingly immobile (Hartholt et al., 1996), apparently making lasting contact in a grid-like structure, through which momentum exchange can take place for instance as a fluidization bubble moves in the vicinity, or in response to some other

stirring action in the bed. Further statistical analysis of the data from the different experiments may make it possible to make further statements about the issue of fast, short-range particle movement.

The data in the top part of Figure 3 show a regular particle circulation in the axial direction. The upward velocity is roughly consistent with the velocity of individual fluidization bubbles, but the downwards motion is – although slower than the upward motion – far higher than one might expect if it is only the result bulk motion compensating for the material removed close to the distributor in bubble wakes.

Figure 4, B shows, as mentioned above, that the starting points of upward particle motion are not uniformly distributed over the bed cross-section. At the same time it is clear from Figure 3 that the pattern in the axial motion is associated with a more irregular, but clearly distinguishable, pattern of motion in the lateral direction. Observing, for instance, the motion around 80000 ms, the particle performs a lateral motion to higher x-coordinate, and conversely at the top of the bed. Moreover, the extremes in axial position seem to be associated with the maximal lateral velocity.

This is all consistent with the notion of “gulf-streaming” in the bed, a phenomenon described, for instance, in Merry and Davidson (1973): Due to cross-sectionally non-uniform bubble flow, the bed consists of a region of high bubble intensity, where the flow of the bed material is upwards driven by the bubble motion, and a region of low bubble intensity, where the bed motion is downwards. Because of this effect much more bed material is brought to the top of the bed by the bubble flow than would be expected from the flow in the bubble wake phase itself, and, consequently, the compensating downward motion is also higher than expected.

Gulf-streaming will cause the fluidization bubbles to move faster than one would expect from the single bubble velocity, on the other hand a certain slip between the bubbles and the dense phase in the region of upward motion can be expected.

Further analysis of the data in the time to come will reveal whether this is, in fact, the right interpretation of the motion we are seeing, and will result in more detailed information about the nature of the particle motion, and the mechanisms behind it. The fact that the aeration of the bed is not uniform is not bad for the information flow from the experiment, rather the contrary: non-uniform aeration of fluidized beds is very common both in the laboratory and industrially.

## 5 REFERENCES

- DECHSIRI C., VAN DER ZWAN E., BOSMA, J.C, PAANS A.M.J. AND HOFFMANN A.C. (2002) "Positron Emission Tomography (PET) for fluidization" *Proceedings WCPT4, the Fourth World Congress on Particle Technology*, Sydney.
- HARTHOLT, G.P., HOFFMANN, A.C. AND JANSSEN, L.P.B.M. (1996) "Visual observation of individual particle behaviour in gas and liquid fluidized beds" *Powder Technol.* 88, 341-345.
- KENDALL, M.G. (1985) "Time-Series" 2<sup>nd</sup> edition, Charles Griffin & Co. Ltd., London
- MERRY, J.M.D. and DAVIDSON, J.F. (1973) "Gulf-stream circulation in shallow fluidized-beds" *Trans. Instn. Chem. Engrs* 81, 361-368.
- SNIEDERS, F.F., HOFFMANN, A.C., CHEESMAN, D., YATES, J.G., STEIN, M. AND SEVILLE, J.P.K. (1999), The dynamics of large particles in a four-compartment interconnected fluidized bed" *Powder Technol.*, 101, pp. 229-239.
- STEIN M., DING YL, SEVILLE J.P.K AND PARKER D.J. "Solids motion in bubbling gas fluidized beds" *Chem. Eng. Sci.* 55, pp. 5291-5300